A

LocateMe: Magnetic Fields Based Indoor Localization Using Smartphones

Kalyan Pathapati Subbu, Brandon Gozick, Ram Dantu, University of North Texas

Fine grained localization is extremely important to accurately locate a user indoors. Although innovative solutions have already been proposed, there is no solution that is universally accepted, easily implemented, user centric and most importantly work in the absence of GSM coverage or WiFi availability. The advent of sensor rich smartphones has paved a way to develop a solution that can cater to these requirements.

By employing a smartphone's built-in magnetic field sensor, magnetic signatures were collected inside buildings. These signatures displayed a uniqueness in their patterns due to the presence of different kinds of pillars, doors, elevators etc., that consist of ferromagnetic materials like steel or iron. We theoretically analyze the cause of this uniqueness and then present an indoor localization solution by classifying signatures based on their patterns. However, to account for user walking speed variations so as to provide an application usable to a variety of users, we follow a dynamic time warping based approach that is known to work on similar signals irrespective of their variations in the time axis.

Our approach resulted in localization distances of approximately 2m-6m with accuracies between 80-100% implying that it is sufficient to walk short distances across hallways to be located by the smartphone. The implementation of the application on different smartphones yielded response times of less than 5 secs thereby validating the feasibility of our approach and making it a viable solution.

Categories and Subject Descriptors: I.5.2 [**Pattern Recognition**]: Design Methodology—*Classier design and evaluation*; I.2.10 [**Artificial Intelligence**]: Learning; J.2 [**Computer Applications**]: Physical Science and Engineering—*Physics*

General Terms: Algorithms, Design, Experimentation, Human factors, Measurement, Performance,Theory

Additional Key Words and Phrases: Indoor localization; Magnetic fields; Smartphones; Ubiquitous

ACM Reference Format:
Subbu K.P., Gozick, B., and Dantu, R. 2012. LocateMe: Magnetic Fields Based Indoor Localization Using Smartphones, ACM Trans. Intell. Syst. Technol. , , Article , 28 pages. ACM Trans. Intell. Syst. Technol. V, N, Article A (January YYYY), 27 pages.
DOI = 10.1145/0000000.0000000 http://doi.acm.org/10.1145/0000000.0000000

1. INTRODUCTION

Indoor localization has been a well known problem for which numerous solutions ranging from infrastructure based to wearable sensor based and now smartphone based have been proposed. The rapid growth of smartphones in today's market has increased the ubiquitous nature of these devices to a great extent. Embedded with GPS, microphones, cameras, accelerometers and magnetic field sensors, they provide ample

This work is partially supported by the National Science Foundation under grants CNS-0627754, CNS-0619871 and CNS-0551694.
Author's addresses: Kalyan Pathapati Subbu, and Brandon Gozick, and Ram Dantu, Computer Science Department, University of North Texas, Denton, Texas, 76203. Prof. Ram Dantu, is currently a visiting professor at the Massachusetts Institute of Technology (MIT). emails : kp0124@unt.edu, brandongozick@my.unt.edu, rdantu@unt.edu.

DOI 10.1145/0000000.0000000 http://doi.acm.org/10.1145/0000000.0000000

means to develop innovative solutions for this problem. GPS is already being used for outdoor localization and navigation [Zheng and Xie 2011]. However, it does not function indoors due to signal attenuation and interference. WiFi based systems assume ubiquitous availability [Cheng et al. 2005; Evennou and Marx 2006], may have device compatibility and authentication issues. Accelerometers [Ofstad et al. 2008], microphones [Pathapati-Subbu et al. 2009] and a combination of these sensors along with WiFi [Azizyan and Choudhury 2009] have also been used for localization. However, no work has utilized the built-in magnetic field sensor for this purpose.

Ambient magnetic fields indoors comprise of disturbances in the Earth's magnetic field that is present everywhere, caused by the ferromagnetic nature [Yamazaki et al. 2003] of steel structures [Burnett and Yaping 2002]. These disturbances [Roetenberg et al. 2003] fluctuate the compass heading thereby resulting in incorrect direction and location information. The heading or the direction using these magnetic fields was estimated in [Afzal and Renaudin 2011] with mathematical error correction mechanisms. Instead of developing compensating mechanisms for this issue, work in [Haverinen and Kemppainen 2009; Storms and Raquet 2009] used external sensors and robots to collect these ambient magnetic fields along different hallways and showed that their uniqueness due to the presence of different kinds of pillars, doors and elevators could be exploited as a solution for indoor localization. However, they do not provide any quantitative reasoning for the occurrence and uniqueness of the signatures. So rather than merely stating that steel structures cause disturbances in the Earth's field, we analytically show *the impact of these structures on the Earth's field by modeling the magnetic field distribution of different kinds and sizes of pillars, doors and elevators*. With this modeling we show how and why magnetic signatures appear the way they are. Also, factors like usability, applicability to different users, and practical implementation have not been considered in their work.

To the best of our knowledge, no work in the literature has utilized the embedded magnetic field sensor as a magnetometer to capture these signatures and utilize them for localization. Work in [Subbu et al. 2011] showed the possibility of performing coarse localization using magnetic signatures entirely on a smartphone. We extend this work to provide finer location information instead of just the hallway name. We envision a scenario where *a user walks a few meters in an unknown hallway, then uses a smartphone to identify his position in that hallway based on the magnetic signature collected for the distance walked.* To brief up the idea, we first fingerprint each hallway using the measured magnetic signature. Then, by classifying the test signature of an unknown hallway to one of the fingerprints, we obtain the person's position in meters, thereby providing fine grained localization. Differences in human walking speeds cause variations in the time and magnitude of signatures, even if they retain the same pattern. Therefore, we incorporate the dynamic time warping (DTW) classifier which is known to account for these differences and perform alignment by stretching or compressing the signals. Our contributions lie in:

(1) Analytically modeling ferromagnetic structures:
In Section 4, we implement an analytical model to quantify the magnetic field distribution or magnetic field behavior of steel reinforced concrete, solid steel pillars, elevators and doors, found in hallways and explain the cause for uniqueness of the magnetic signatures.
(2) Developing an application encapsulated in a single sensing unit:
The localization application requires no external device or infrastructure, is position and orientation invariant and can work over a variety of users.
(3) Presenting an application that can be used in a realistic setting with real users:

In Section 6, our classification and evaluation results across 10 hallways in two different buildings yielded classification accuracies between *81-99%*, localization distances of less than $6.5m$ and estimation errors of less than $4m$. The implication of the results discussed in Section 7 shows that our application can be deployed on smartphones with different magnetic field sensors and processing capabilities.

2. EMPIRICAL SETUP

In this section, we briefly discuss the hardware and software platform, and the data collection procedure followed for obtaining the magnetic signatures.

2.1. Smartphone platform

We employed a HTC Nexus One smartphone with a 1GHz Snapdragon ARMv7 processor and 512MB of RAM. It has a built-in 3-axis AK8973 monolithic geomagnetic sensor or magnetometer, manufactured by Asahi Kasei [AK]. The sensor is capable of providing a dynamic sampling frequency, meaning the number of samples recorded per second can be changed using the API's offered in the Android [And] operating system. By choosing a sampling rate, we can control the number of samples recorded by the sensor which has great influence on both the power consumption and also the amount of processing time needed for computations.

The smartphone runs on Android operating system which has an easy development environment and access to hardware level application programming interfaces (APIs). With this, we can create a smartphone application that is both practical and user friendly.

2.2. Data collection

The fingerprints were collected in different hallways of two campus buildings, University Union and College of Engineering (COE). The floor maps in Figures 1(a) and 1(b) illustrate the different hallways.

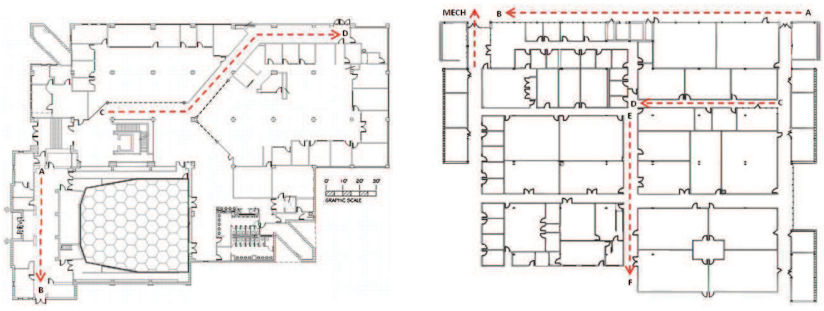

(a) (b)

Fig. 1. The paths AB, CD, EF and Mech, show the hallways where data collection and system evaluation were performed.

Table I summarizes some experimental specifications showing the number of hallways (N_{hwys}), number of fingerprint repetitions (F_r), average hallway length (HL_{avg}), total training file size (Tr_{fs}) and time consumed for data collection (T_c) in each of the buildings.

Both the subjects walked with an average speed of 1.5m/s along the walls or pillars for three main reasons 1) to obtain a dominant signature that could arise due to walls

Table I. Data collection statistics .

	Union	COE
N_{hwys}	6	4
F_r	10	15
HL_{avg}	38m	51m
Tr_{fs}	12Kb	8Kb
T_c	40 mins	68 mins

and ferromagnetic objects 2) mimic usual walking patterns of people and 3) make the application useful for visually impaired people who follow a wall trailing [Hill and Punder 1976] procedure where they walk past walls holding or sensing the touch of objects such as pillars, doors, walls etc. A simple description of the walking process is depicted in the video [Loc].

3. CHALLENGES

This section discusses factors such as variations in a)the built-in sensors, b) measurement procedure and c) the environment that could potentially affect the stability of the magnetic signatures.

— *Built-in sensor model variation:* Different smartphones consist of different models of built-in magnetic field sensors that vary in their sensitivities. For our system to work, it is imperative that the magnetic signatures collected at the same location show similarity. To check this similarity, we employed four phones with different magnetic field sensors. Table II lists the phones and the model number of the built-in sensors.

Table II. Smartphones and their built-in sensor model characteristics

Phone	Sensor Model	Sensitivity(μT)	Resolution(μT)
Nexus One	AK-8973	2000	0.0625
Captivate	MS-3C	1200	0.585
Epic 4G SII	AK-8975	2000	0.06
Galaxy Nexus	MPL	8001	0.012

The data was collected using all the four phones one after the other. Figure 2 shows the signature of Electrical Engineering hallway recorded using the four phones.

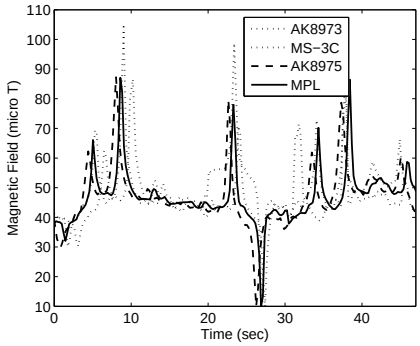

Fig. 2. Similarity of signatures captured using four smartphones with different sensors.

— *Measurement Process:* The measurement process in this work is simply to walk past pillars along the hallway. However, care has to be taken to walk closer to the pillars since magnetic field magnitudes are known to be inversely proportional to the cube of the distance. In other words, the farther the distance from an object, the lower the magnitude. To observe if this phenomenon affected the signatures, measurements were made at different horizontal distances from walls and pillars. This gives an idea of how far can users walk and still be able to obtain a satisfactory signature. Figure 3 illustrates this observation.

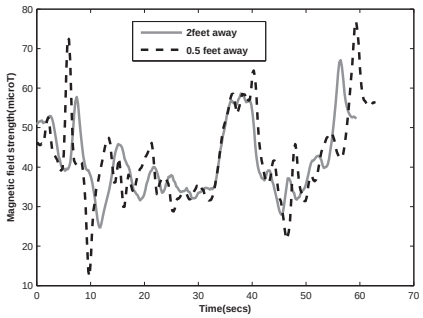

Fig. 3. It can be seen that for the data 2 feet away, the magnitude is reduced as compared to that from 0.5 feet away but the patterns are still similar.

— *Device placement:* Since we are only considering the overall squared magnitude of the magnetic field and not the magnitude of individual axes, the placement of the phone should not cause any problems in our work. To verify this, we collected data with the phone at different locations. Figure 4 illustrates the findings.

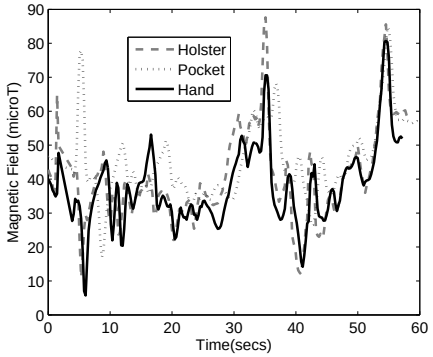

Fig. 4. Signatures obtained by placing the smartphone in a holster, pocket, and holding in the hand.

— *Presence of furniture:* The other factor that we speculated would affect the magnetic signatures is the presence of furnitures along hallways. To test this speculation, we collected data in the presence and absence of furniture in certain hallways. Figure 5 below shows the signatures obtained with a chair and table placed at different spots along the hallway. As can be seen, there is not much difference in the two signatures. The furniture experimented with was chairs with metal support and wooden tables. Unless the furniture consists of heavy metallic objects that are frequently replaced,

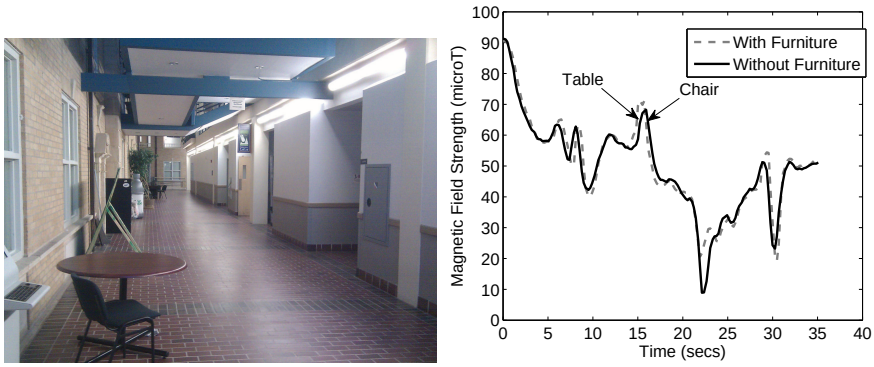

(a) (b)

Fig. 5. Effect of furniture on the signature: (a) Shows the commonly present movable furniture. (b) Magnetic signatures collected in the presence and absence of furniture. There is no drastic effect on the signature.

we believe there would not be any issue with the system since finding such equipment was a difficult task to fulfill. We therefore found similar objects which might be realistically placed and then removed inside a hallway.

— *Presence of personal metallic objects:* We also tested the affect of magnetic signatures due to the presence of small metallic objects in the user's pocket along with the smartphone. In other words, we wanted to find if the magnetic field sensor was disturbed by common items carried by people in their pockets thereby drastically changing the magnetic signatures collected. Figures 6 show signatures obtained from three separate measurement processes involving a key chain, loose change and a flash drive placed along with the phone in the pocket. Again, we can see that pres-

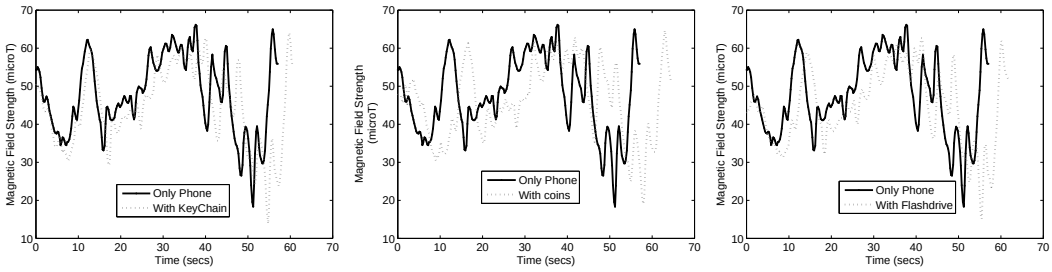

(a) (b) (c)

Fig. 6. Effect of metallic objects: (a) A set of keys in a keychain (b) Loose change (c) A flash drive in the pocket.

ence of various objects in the pocket along with the phone did not cause any major effect on the signature other than a time delay due to different walking speeds) and magnitude variations due to (distance from wall) which the dynamic time warping algorithm is capable of matching.

— *Long term variation:* Similar to variations in the sensors and variations in the measurement process, long term variations in the environment itself could be a cause for changes in the magnetic signatures. Long term variation is the change in the magnetic field magnitudes over a certain period of time. To check if this phenomenon

was present in the signatures, we computed the variance of the magnetic signature of a particular hallway collected over a year. Figure 7 depicts this observation.

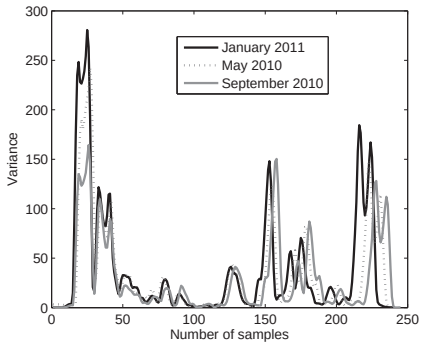

Fig. 7. The variance of magnetic signature of a same hallway collected during different months. As can be seen, there is no major variation in all the signatures that could render it ineffective for our solution.

4. MAGNETIC ANOMALIES

In this section, we provide an analytical reasoning for the occurrence and uniqueness of magnetic signatures observed and then extend the modeling to a simulation framework that can be used to generate magnetic signatures of various hallways with different kinds of pillars, elevators and other ferromagnetic objects present.

4.1. Perturbations in Earth's Magnetic field

Indoor magnetic signatures are a combination of the Earth's magnetic field and the fields from ferromagnetic objects such as pillars, doors and elevators. These signatures are known as anomalies because they disturb the Earth's magnetic field.

The Earth acts like a great spherical magnet, surrounded by a magnetic field [Oldenburg and Moridis 1998] which changes both with time and location and resembles the field generated by a tilted dipole magnet whose axis is offset from the axis of the Earth's rotation by approximately 11°. The Earth's magnetic field can be generated using the IGRF-International Geomagnetic Reference Field model [IGR] released by International Association of Geomagnetism and Aeronomy (IAGA). The model generated Earth's magnetic field was compared with the field measured at five different locations depicted in Figure 8.

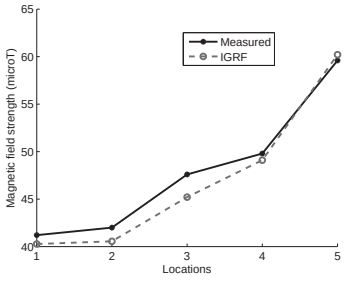

Fig. 8. Comparison of generated and measured Earth's magnetic field: A correlation of 99.5 was obtained from above data.

However, as we know, in indoor environments, the Earth's magnetic field is disturbed by structures made of ferromagnetic materials. The impact of these structures becomes dominant as the distance to the observation point decreases or in other words distance towards the pillar decreases. This impact can be observed in Figure 9 below.

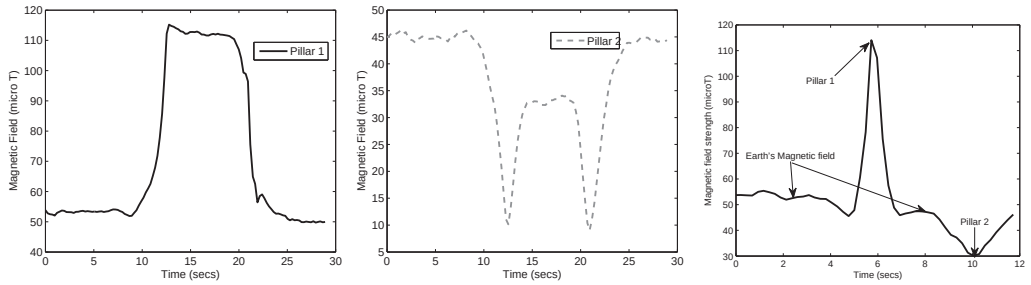

(a) (b) (c)

Fig. 9. Impact on Earth's field: For the first and last 10 secs, there is no major change in the Earth's magnetic field. As the distance towards the pillar decreased, the magnitude changed drastically to (a) A high value of 115μT at one pillar (b) A low value of 33μT at another pillar. (c) The high and low magnetic disturbance caused by the two pillars are clearly indicated along with the Earth's field until 4.3 secs and then between 6.5-8.3 secs approximately.

4.2. Pillars

The COE and Union buildings consist of solid steel and steel reinforced concrete pillars respectively. The magnitudes of the signatures in the two buildings varied between $35 - 115$ μT and $100 - 220$ μT respectively. This showed that steel reinforced concrete pillars caused stronger disturbances on the Earth's magnetic field than solid steel pillars. To understand this observation, we implemented an analytical model to generate magnetic signatures in the presence of these pillars and compared them with the measured data.

We followed the point dipole model [Jackson 1999] given by Equation 1.

$$B(\vec{m}, \vec{r}) = \frac{\mu}{4 * pi}[3\frac{(\vec{m}.\vec{r})\vec{r}}{|\vec{r}|^5} - \frac{\vec{m}}{|\vec{r}|^3}] \tag{1}$$

where μ is permeability of free space, $\vec{m}$ denotes the magnetic moment, which is the average field strength at any particular point, also known as saturation magnetization and $\vec{r}$ is the distance between the dipole and the observation point. The resultant moment arising due to the interaction of multiple dipoles is given by

$$M_{total} = \sqrt{m_1^2 + m_2^2 + m_1.m_2 \cos\phi} \tag{2}$$

with ϕ being the angle between the dipoles and m_1 and m_2 the magnetic moments of the two interacting dipoles. By substituting M_{total} in Eq. 1, the magnetic field was obtained for both steel reinforced concrete and solid steel pillars.

(1) Steel Reinforced Concrete: Typically, steel reinforced concrete pillars are constructed by first forming a grid like structure of steel rods or rebars tied together [E.Čermáková 2005; Craig M. Newtson 1995]. The rods are equally spaced to form either a cylindrical grid for a cylindrical pillar or a rectangular grid for a rectangular pillar shown in Figure 10. By calculating the combined or coupled dipole moment due to parallel and perpendicular dipoles or rebars [Kristjansson

(a) (b)

Fig. 10. Type of grids. (a) Cylindrical grid (b) Rectangular grid

1983] using Eq. 2, the resulting magnetic field distribution of a particular grid size was computed using Eq. 1. Figure 11 shows the analytical and measured magnetic field changes in the Earth's magnetic field due to the magnetic field interaction of cylindrical and rectangular grids. The model was implemented by assuming a person walking past the pillars. This should show a rise and drop in the magnetic field as the distance to the pillars changes.

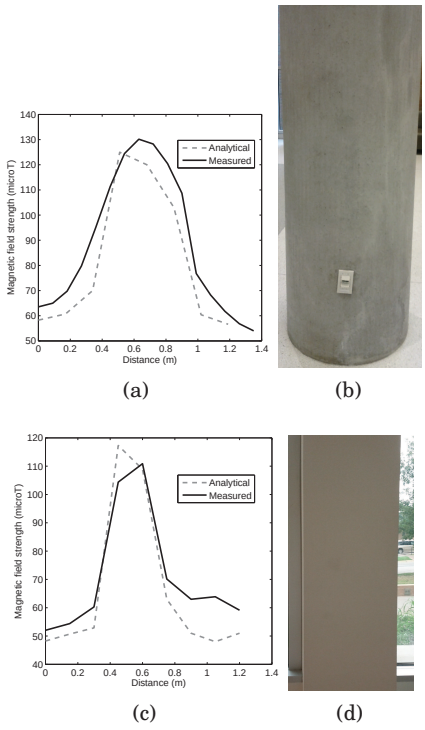

Fig. 11. Analytical and Measured magnetic field disturbances due to reinforced pillars. (a) Cylindrical grid size of 2.5x2.5 foot. (b) A typical cylindrical steel reinforced pillar. (c) Rectangular grid size of 2.5x2.5foot. (d) A rectangular steel reinforced pillar.

(2) Solid Steel: Now, using the same model, the pillars at the COE were considered as a single dipole since they were solid steel structures and did not contain multiple steel rods. Figure 12 illustrates the analytical and measured distributions.

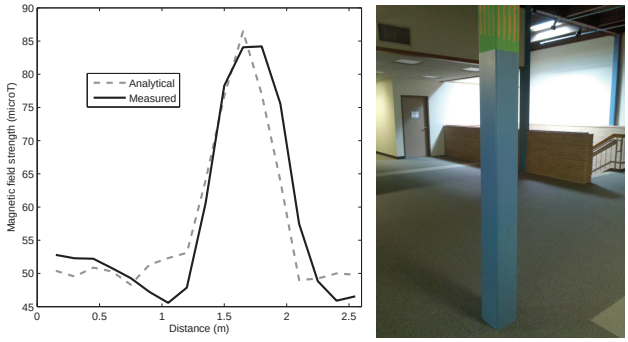

(a) (b)

Fig. 12. Magnetic field distribution of a solid steel structure. (a) Analytical and Measured (b) Solid steel pillar

Figures 11 and 12 confirm that the disturbance of steel reinforced concrete pillars on the Earth's magnetic field is stronger than solid steel pillars due to the presence of multiple steel rods and dipolar interaction.

4.3. Simulation Framework

The previous sections explained the ferromagnetic phenomenon observed from the collected magnetic signatures. To extend this analytical modeling, we performed simulations to generate magnetic signatures assuming either steel reinforced or solid steel pillars, doors, and elevators present along hallways of different lengths. The motive behind this simulation was to validate the classification algorithm that will be explained in Section 5 on various kinds of hallways since data collection over all possible hallways is not possible for the evaluation of the proposed system. The simulation methodology consisted of following steps:

(1) Consider a geometrical shape, for instance, a cube for a solid pillar as seen in the COE building with dimensions given in the table below.

Table III. Different pillars: Dimensions in cm.

Type	a (cm)	b (cm)	h (cm)
Solid(corner)	20	20	500
Solid(middle)	20	20	500
H-Shape	10	11	500
Solid(small)	15	15	500

(2) Next, the magnetic moment of the pillar was calculated as

$$\mu_{pillar} = (\mu_{atom})(N_{atoms}) \tag{3}$$

where the number of atoms N_{atoms} was computed as

$$N_{atoms} = \frac{(Fe_{den})(V)}{(L)(A_{mass})} \tag{4}$$

with Fe_{den} being the density of $1m^3$ of iron given as 7.87×10^3 kgm^{-3} and A_{mass} is the atomic mass given as 92.711×10^{-27} kg and L is the Avagadro's number given by 6.22×10^{23}.

(3) The magnetic moment in the pillar varied depending upon the number of atoms aligned [E.Čermáková 2005]. Hence, the moment was varied as

$$\mu_{pillar} = (N_{aligned})(\mu_{pillar}) \tag{5}$$

(4) Next, the magnetic field of the pillar was calculated using Eq. 1.
(5) Finally a signature as shown in Figure 13 was obtained assuming a person walking in a hypothetical hallway consisting of six pillars.

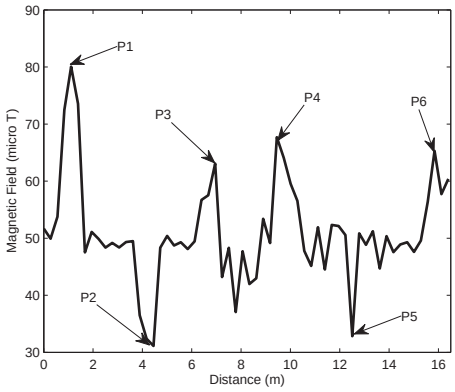

Fig. 13. Generated magnetic signature: The highs and lows of magnetic fields that were observed in the measured signatures can be seen at each of the pillars

We clarify here that a quantitative comparison between the measured and simulated magnetic signatures between existing hallways cannot be performed due to the presence of unknown variables such as the exact make or type of iron used in the pillars, their properties etc. The idea behind generating such signatures will be understood in Section 6 where we show how these generated signatures are used for validating the dynamic time warping classifier.

4.4. Door Frames

Doors are other elements that constitute ferromagnetic materials. There are different kinds of doors present in hallways. Our magnetic signature collection process revealed that door frames were made of steel and this resulted in patterns identifiable along hallways making it feasible to detect the door a person is close to while walking in a hallway. Figure 14 illustrates this finding.

The analytical implementation of the door signatures was performed by using the dipole model and considering each frame in the door as a ferromagnetic object. Figure 15 depicts both the analytical and measured signatures of a door.

In Section 6, we present classification results of this particular door i.e F226 along a hallway. To conclude, this section provided an understanding of the ferromagnetism phenomenon and the magnetic behavior of different kinds of pillars, doors and elevators and their effect on the Earth's magnetic field. The next section briefly explains the classification algorithm that forms the backbone of this location identification system.

5. CLASSIFICATION SYSTEM

The previous section explained the reason behind obtaining unique magnetic signatures. In this section, we transition to the application domain and explain the classi-

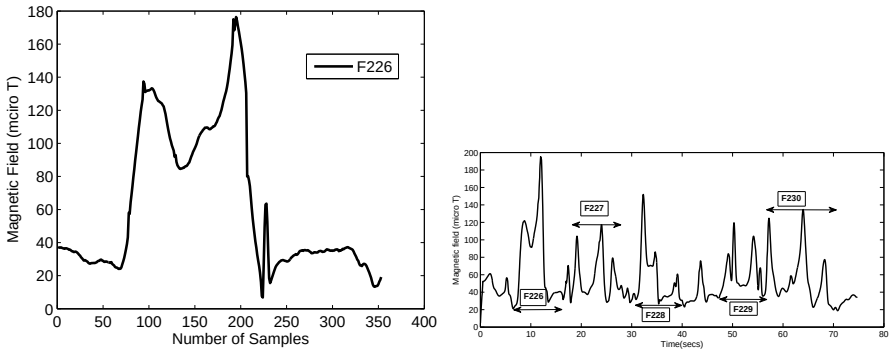

Fig. 14. Door identification. (a) The door shown consists of three frames, one at the start and the other two corresponding to the start and end of the window section. (b) shows the hallway with different doors and the door in (a) clearly identified by the marker.

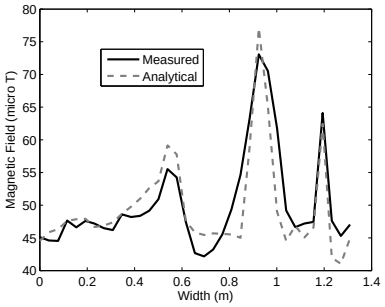

Fig. 15. Analytical and Measured signature of a door.

fication technique implemented on the measured signatures. We start with the DTW algorithm and its applicability to indoor localization and then the procedure for localizing and estimating the distance walked using DTW on the magnetic signatures.

5.1. Dynamic Time Warping

The technique in DTW is to compress or stretch the time axis of one (or both) sequences to achieve a better alignment. In general, consider two signatures, $T = \{t_1, t_2, ..., t_A\}$ and $S = \{s_1, s_2, ..., s_B\}$ of different lengths. The goal is to find the best match between the two signatures by some alignment w, the optimal warping path. The warping path is given by $w = w(1), w(2), ..., w(n)$, where $w(n) = [i(n), j(n)]$ is the set of matched samples, where i and j corresponding to the time axes of two sequences respectively. The objective of the warping function is to minimize the overall cost function given by

$$D = \sum_{n=1}^{N} \delta(w(n)) \tag{6}$$

where $\delta(w(n))$ is the squared distance between the sample points given by

$$\delta(w(n)) = (i(n) - j(n))^2 \tag{7}$$

The warping path must satisfy the following constraints:

— Monotonicity: The warping path must progress in the forward direction, i.e $i(n) \geq i(n-1)$ and $j(n) \geq j(n-1)$, where $w(n-1) = [i(n-1), j(n-1)]$ and $w(n) = [i(n), j(n)]$.
— Boundary: The function must always start at $w(1) = (1, 1)$ and end at $w(n) = (A, B)$
— The function must not skip any points, i.e $i(n) - i(n-1) \leq 1$ and $j(n) - j(n-1) \leq 1$

To generate a warping path, a cost matrix is constructed. This matrix represents the minimum cost required to reach a particular point (i, j) from $(1, 1)$. This minimization problem is usually solved using the dynamic programming approach, whereby a cumulative or accumulated distance $\gamma(i, j)$ is computed as the sum of $\delta(w(n))$, the distance obtained from the current set of points and the minimum of the cumulative distances of the adjacent elements or neighbors. This is given by

$$\gamma(i,j) = \delta(w(n)) + min[\gamma(i-1,j) \\ ,\gamma(i-1,j-1) \\ ,\gamma(i,j-1)] \tag{8}$$

After performing the time warping, the closest match is obtained by the lowest cumulative distance between the signatures.

5.2. Estimating localization distance using sliding windowed DTW

Instead of classifying the test signature of an entire hallway as in [Subbu et al. 2011], we performed DTW between a short test signature and stored signatures. (For the remaining sections, we will refer to stored signatures as maps). To compare the short signature, we implemented a sliding windowed DTW explained in Figure 16.

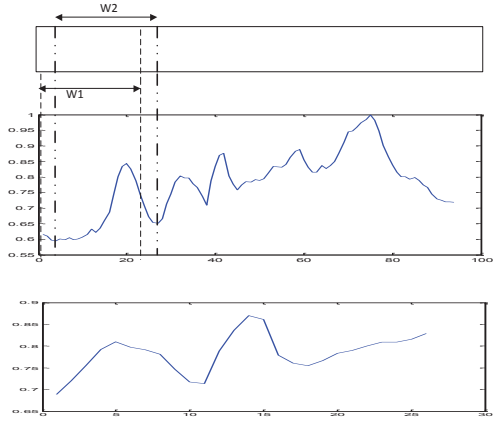

Fig. 16. A test signature (below) and map (above) denoted by $T_e = \{te_1, te_2, ..., te_n\}$, and $M = \{m_1, m_2, ..., m_m\}$, respectively. Using a sliding window on M, T_e is compared with segments of the map, $\{M_a ... M_m\}$, $\{M_{a+1} ... M_{m+1}\}$ corresponding to $W1$ and $W2$, of width equal to W_l, the window length in samples.

Our program picked 100 random positions from each test signature and performed classification for each of those positions. This was mimicking the procedure of obtaining a signature when a person walks for a short distance. The randomly picked segments were of length equal to W_l which ranged between 5 and 35. In simple terms, W_l is nothing but the *resolution or shortest distance* required to walk in a particular

hallway to get localized. We basically tested different resolutions to see which one was the best for each hallway. The DTW was performed between each short test segment and sliding windowed segments of the maps.

The classification accuracy was calculated as

$$A = \#Correctmatches/100 \tag{9}$$

Then using the sampling rate s_r and W_l, the time taken to walk a certain distance t was calculated as W_l/s_r. The distance for the stored maps was calculated using δ=$v * t$, where v is the velocity. The localized or estimated distance was obtained from the section of the stored maps where DTW correctly matched the test signature. The estimation error for every W_l was calculated as $E = \delta_M - \delta_E$, where δ_M is the distance measured manually using a surveyor's wheel. Finally, the average estimation error σ_e over all positions for a particular W_l was calculated.

6. RESULTS

In this section, we discuss the performance of the classification algorithm on both the measured and simulated magnetic signatures. We also discuss the response or result computation times, memory and power consumption of the algorithm when run as a stand-alone application on different smartphones.

6.1. DTW Performance

6.1.1. Alignment Evaluation. Figure 17 illustrates the sliding windowed DTW on the measurement data. Short segments of a test signature were randomly picked as explained in Section 5.2 and DTW aligned these segments with an appropriate windowed segment of the map, thereby matching the test signatures correctly to the respective map or hallway.

6.1.2. Independence of phones and sensors. In Section 3 we showed visually the similarity of signatures collected from smartphones with different magnetic field sensors. Here we show the performance of DTW in classifying such magnetic signatures, indicating the independence of our system on devices.

A total of 16 test signatures were obtained from four subjects each using a different phone listed in Table II. The windowed DTW was performed on each of these test signatures for random number of positions or short segments of size 35 samples. Figure 18 illustrates the matching process. The signature obtained from Galaxy Nexus which has the MPL magnetic field sensor was considered as the training signature or the map and the signatures from the other phones were tested against this signature for a correct match. From the plots, we can see that DTW classifies signatures irrespective of the sensor sensing the magnetic fields. The classification accuracies were computed as A = N_P / T_P and listed in Table IV below, where N_P and T_P are number of correctly matched positions and total number of positions respectively.

Table IV. Classification accuracies for phones with different built-in sensors

Phone	Sensor Model	CSE (%)	EE (%)
Nexus One	AK-8973	90	91
Captivate	MS-3C	88	87
Epic 4G SII	AK-8975	94	93
Galaxy Nexus	MPL	92	89

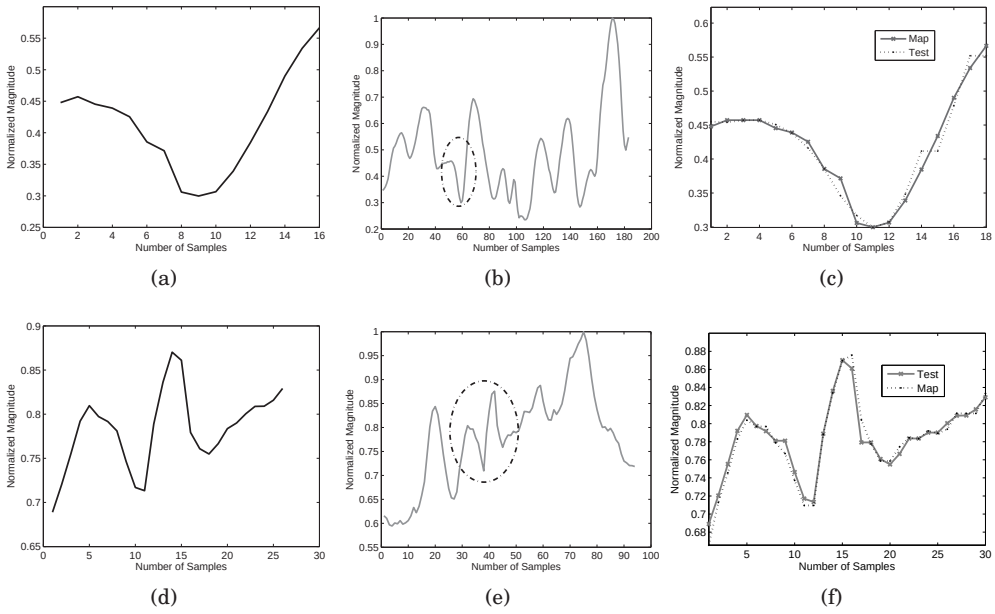

Fig. 17. Alignment by DTW: Short test signatures (a) and (d) are compared with windowed segments from maps (b) and (e) to obtain correct matches as (c) and (f) respectively (the correctly matched segments are marked by an ellipse in the maps. Finally, the distance walked is estimated by using the sample number at which the match was obtained explained in Section 5.2).

6.2. Estimation error and Localization distance

We performed both Matlab (offline) and Smartphone (online) based evaluations to obtain the estimation error and localization distances. For offline evaluation, we gathered a database for each building which had one stored signature map for each hallway in the building. The estimation error was computed as explained in Section 5.2 for each random position and averaged. Figure 19 depicts the average estimation errors computed offline over all the positions chosen for every window size (resolution) in the University Union building.

We can see that for five out of the six hallways, the error is between 0 and 3.5m approximately. There are some outliers such as 25.2m for a W_l of five samples in the ESSCLvL2 and 17m for 15 samples in the Bookstore hallways. The reason for this is very low resolution in those particular hallways for which DTW was unable to obtain a correct match. Moreover, there could have been segments of signatures that had a similar pattern as that of the test which resulted in the DTW performing a wrong match. However, for the remaining window sizes, the error reduced to within 2m and 5m respectively for the two hallways.

Next, we developed the entire application *Locate Me* on the smartphone. The application was written in Java using Android APIs. It has three components: sensor sampling rate identifier, test signature collector, and hallway classifier. The sampling rate identifier calculates the frequency of the magnetic field sensor in the Android phone being used. During our preliminary data collection, we noticed that different smartphones had different sampling rates. For this application to function properly, it is required to find the sampling rates in the phones. This process is performed automatically once the application is opened and requires no user interaction to complete (no user requirements). The splash screen shown in Figure 20(a) performs this analysis. Finding

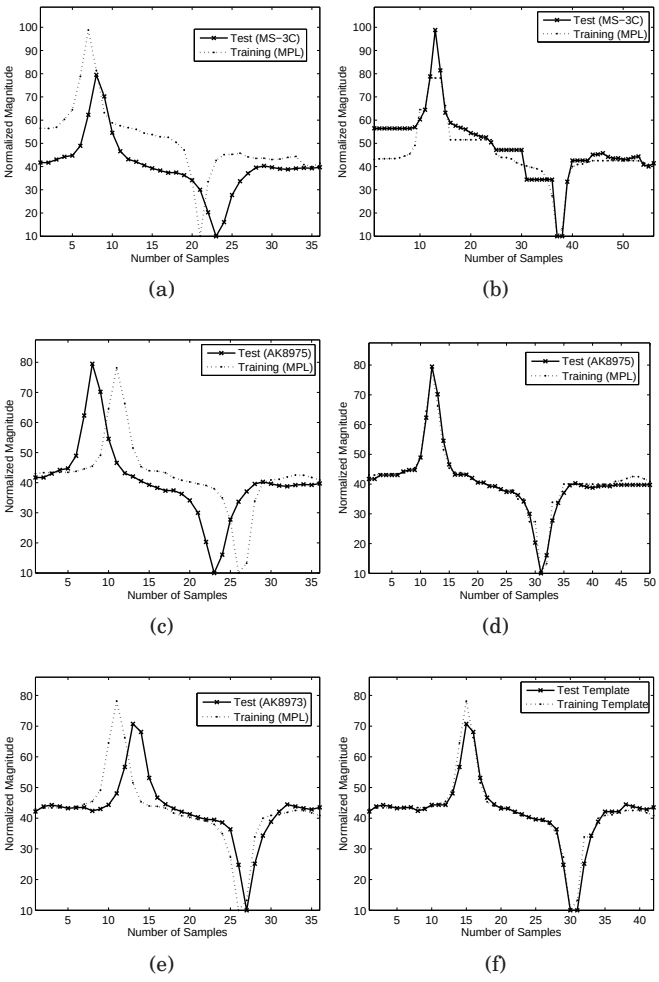

Fig. 18. DTW performance: (a),(c) and (e) are the original test signatures recorded using MS-3C, AK-8975 and AK-8973 sensors. (b),(d) and (f) show the matching process.

this rate allows consistency in functionality and an accurate hallway match. The other components and the complete user interface of the application is shown below.

Figure 20(b) shows the home screen for the LocateMe application. This screen contains the building selection drop down list. The user, assuming he/she knows which building they are in (can also be obtained using GPS just before entering), picks the building from the list. This list is shown in Figure 20(c). Magnetic maps for the corresponding building are then downloaded onto the phone. The localization results will reflect the comparison of these stored maps with the test signature collected by the user. The test signature collector obtains the sensor data when the user pushes the Start/Stop toggle button shown in Figure 20(b) and walks a certain distance. An example of test signature collection is shown in Figure 20(d).

For evaluation, we used different set of phones namely Nexus One, Droid, Nexus S, and HTC Hero. We chose 10 users for a total of 10 hallways in two buildings, one user per hallway. Given the lesser number of hallways in the COE building and the

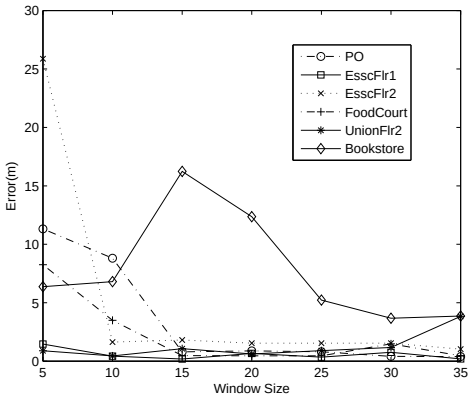

Fig. 19. Estimation errors for University Union as a function of window length or resolution.

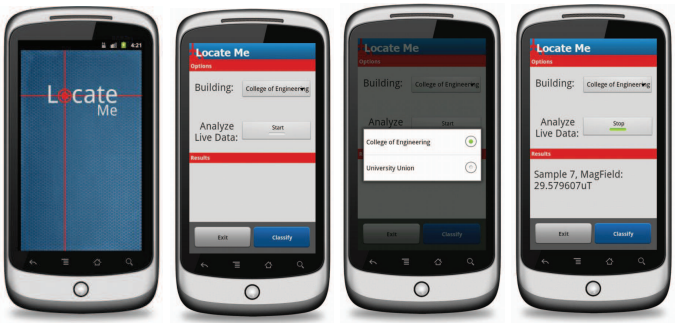

Fig. 20. (a) Splash Screen (sensor frequency analysis) (b) Home Screen (c) Building Selection (d) Capture Live Data

convenient access we had to it, we instructed the users to walk and record random segments of the hallway each starting at different positions. The users therefore walked 26, 15, 13, and 13 different positions in their hallway varying the walking distance each time. A lower total of 10 segments in the Union were subsequently recorded due to inconvenient access and a high afternoon building population. After collecting the test signature, the user pushed the Classify button located at the bottom right corner shown in Figure 20(b). This is when the hallway classifier is activated which in turn activates the classification system block explained in Section 5.

Obtaining similar error plots as Figure 19, we analyzed which particular window size resulted in a high accuracy and low estimation error for a particular hallway. In other words, we picked the lowest resolution that was obtained with a high accuracy and low estimation error for both the offline and online evaluations. We list these statistics in Tables V and VI.

As seen, a 96% accuracy was obtained for Corr2 as 25/26 where 25 is the number of correct matches and 26 is the total number of repetitions.

The tables indicate the resolution (distance required to walk) within certain meters with a certain accuracy obtained from offline (Matlab) and online (smartphone) evaluations. For instance, we can say that it is required to walk 2.32m in Corr2 hallway to be localized within 3m with a 90% accuracy. The smartphone based results were close to the Matlab results thereby validating the evaluation procedure. The slight differ-

Table V. Accuracy (A), Avg estimation error (σ_e (m)) and Avg localization distances (δ_l (m)) for COE

Hallway	Matlab			Smartphone		
	A (%)	σ_e	δ_l	A (%)	σ_e	δ_l
Corr2	90	3.05	2.32	96	3.2	3.4
Corr4	99	3.50	3.43	93	3.6	4.0
Mech	86	3.37	4.57	84	3.7	5.3
CSE	96	0.66	4.57	92	1.2	4.7

Table VI. Accuracy (A), Avg estimation error (σ_e (m)) and Avg localization distances (δ_l (m)) for University Union

Hallway	Matlab			Smartphone		
	A	σ_e	δ_l	A	σ_e	δ_l
Post Office	88	0.79	2.2	90	1.5	3.0
ESSCLvL1	94	0.33	4.57	100	1.1	5.1
ESSCLvL2	81	1.62	1.83	80	1.9	2.1
Foodcourt	93	0.45	3.5	100	0.7	4.2
UnionLvL2	90	1.17	5.5	90	1.3	5.9
Bookstore	87	3.67	6.3	90	4.0	6.5

ences in the results between the two evaluations were due to minor variations in the sensor data collected while experimenting. However, this did not affect the outcome in a major way.

Now, we compare our results with those obtained (tabulated in Table VII) from a particle filter based approach followed in [Haverinen and Kemppainen 2009]. This is the only existing work related to magnetic field based localization with humans. The authors in [Haverinen and Kemppainen 2009] conducted their experiment in main corridors of a floor of total length 278 m. The particle filter simulation program incremented the position of the human by 1m thereby obtaining 278 positions for the entire hallway. Further, each experiment set was conducted using different values of standard deviation σ_r of the measurement model between [1 μT, 5 μT]. The measurement model used was a single variable Gaussian probability density function given by

$$p(z|x) = \frac{1}{\sigma_r\sqrt{2pi}} exp(-\frac{(z - |h(x)|^2)}{2\sigma_r^2}) \tag{10}$$

where x is the state of the system. The magnetic field data captured by a user using a wireless magnetometer was the observation z and function $h(x)$ was used to map x to the observation. In other words, the particle filter compared the z at every instant to the map data (collected by a robot).

Table VII. Avg estimation error(σ_e (m)) and Avg localization distances (δ_l (m))for different σ_r using particle filters

σ_r (μ T)	σ_e (m)	δ_l(m)
1.0	3.47	9.98
3.0	3.46	23.98
5.0	3.43	45.02

From Tables V and VI, we can see that the minimum and maximum localization distance required to walk are 1.83m and 6.3m respectively. Although 6.3m is a large distance for this particular hallway, it was less than 5m for the other hallways. This is a significant improvement over values between 9m and 45m shown in Table VII. The

cause for large localization distances obtained using particle filters can be attributed to the fact that particles take a longer time or distances to converge at a point where there is a minimal deviation between the map and the test signatures. In contrast, the DTW algorithm handles these deviations very well by either stretching or compressing the signatures.

6.3. Response Times on different phones

Response time is the time spent by the user waiting from initially pushing the classify button to the time he/she receives a classification and position estimates. Average response times were calculated for each hallway and summed to obtain a total response time for the building. The response times in seconds, obtained from each smartphone are illustrated in Figure 21.

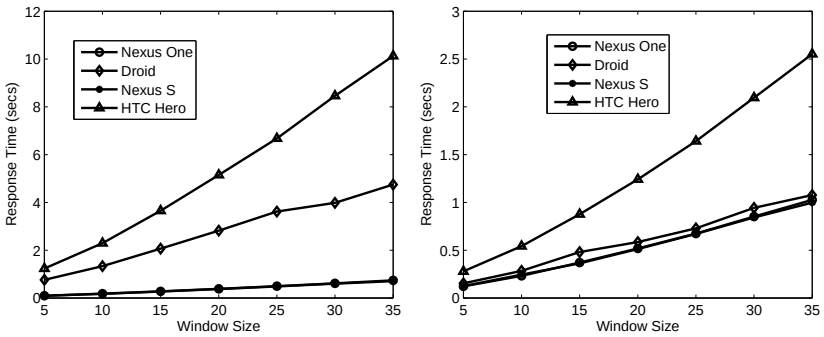

Fig. 21. Relationship between response times and window length for COE (a) and University Union (b) buildings.

The following observations can be made from the above figure:

(1) There was a linear increase in the response times for both buildings. This was due to the inverse proportionality between window length and number of sliding windows. A shorter window length resulted in more windows. This made the DTW perform faster since it had lesser number of samples to classify as compared to a longer one, thereby resulting in faster response times.
(2) The hallways in the University Union had shorter response times when compared to COE. This was because the average length of hallways in COE was greater than University Union as listed in Table I.
(3) Both Nexus One and Nexus S had faster response times when compared to Droid and Hero. This can be correlated with the information from Table VIII, which means *faster the processor, faster the computation time.*

Table VIII. Smartphones and their specifications

Model	Processor Make	Processor Speed	RAM
Nexus One	Qualcomm QSD8250	1GHz	512 MB
Droid	TI OMAP3430	600MHz	256 MB
Nexus S	Cortex A8	1GHz	16GB iNAND flash memory
HTC Hero	Qualcomm MSM7200A	528MHz	288 MB

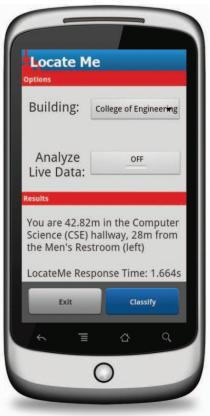

Fig. 22. The screen shows the classified hallway, position of the user in that hallway and from a nearby landmark. The response time of the algorithm is also shown.

A screenshot of the results showing the classification result, distance and response time is illustrated in Figure 22.

In [Gozick et al. 2011], the authors showed how magnetic signatures can be used as landmarks. Using this information, the position of a user near certain landmarks as shown in Figure 22 can be given. There are also other means of extracting landmarks [Millonig and Schechtner 2005] and integrating them with the fine localization results presented in this work.

6.4. Memory and Power Consumption

Android allows external storage up to 32GB which is more than sufficient for storing a set of magnetic maps for each building since the size of the database is very small as listed in Table I.

The amount of resources consumed by the LocateMe application is of primary interest. From the response times shown earlier, it is clear that LocateMe does not require more than 2 minutes for all the three components explained earlier to run. So we compared the memory usage of RAM in mega bytes and power consumed in mill Watts by our application to other activities that normally run on a smartphone for a duration of 2 minutes.

Table IX. Performance - Memory and Power Consumption on Nexus One

Application	Memory (MB)	Power (mW)
Active Call	1.14	327
Game	4.70	556
LocateMe	**6.63**	**480**
Music	13.66	250
Navigation	24.13	600
System	31.78	74

The table shows that LocateMe does not consume much resources and can be run without affecting the functioning of other applications or burdening the CPU.

6.5. Simulation Results

The simulation methodology explained in Section 4.3 was performed assuming hallways of lengths 40-80 m since most of the hallways at which measurements were taken

were normally between this range. For each hallway length, 100 different hallway signatures were generated and the dynamic time warping algorithm was evaluated on each of the 100 signatures. By checking if the closest match was equal to the expected.

The simulation picked 100 random positions from each of the 100 test signatures and performed classification for each of those positions. Fig. 23 illustrates the DTW matching.

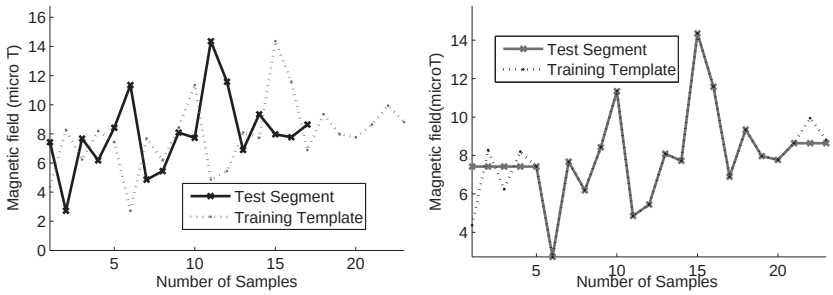

Fig. 23. DTW on synthetic signatures: (a) Training and test signatures. (b) Aligned signatures.

Table X lists the average error and average localization distances obtained for hallways of different lengths generated assuming the presence of pillars, doors and elevators. The distance between each of these objects was assumed to be 4.75m similar to the distances measured in the COE building. The accuracy was computed using Eq. 9 and then an average accuracy was further calculated as Avg_A = A_H/100.

Table X. Avg estimation error(σ_e (m)) and Avg localization distances (δ_l (m))for different length hallways.

H_l	A	σ_e (m)	δ_l(m)
40	93	3.47	3.68
50	92	3.46	3.9
60	91.6	3.7	5.02
70	91	4.43	5.6
80	90	5.5	6.2

6.6. Door Classification

In Section 4.4, we showed that metallic door frames tend to create disturbances thereby resulting in signatures sensed by the smartphone sensor. Here, we show how the door signatures could be identified in a hallway using DTW. Figure 14 depicts two different door signatures and the performance of DTW in classifying them.

7. DISCUSSION

From the results obtained, we showed the applicability of DTW to match signatures collected by different people and provide localization independent of the *user and the device*. The proposed application was also validated with subjects completely new to the buildings and also various kinds of signatures. Hence, it is practically feasible and

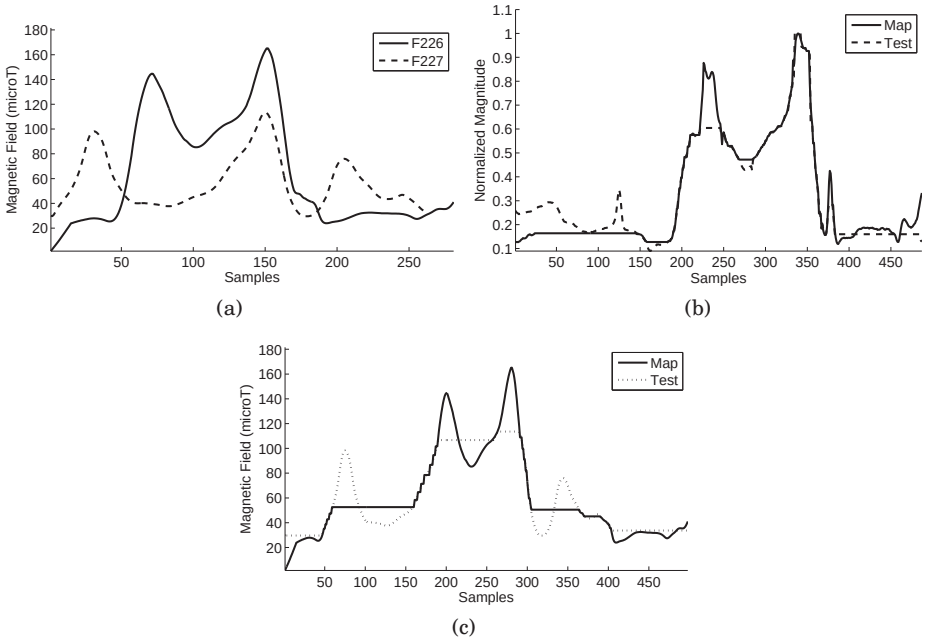

Fig. 24. Door classification. (a) This consists of doors from two different rooms F226 and F227. (c) Although, the signatures look similar, DTW classifies them as being different when compared to (b) which is correctly classified as the same door.

can be used by anyone owning a smartphone (regardless of the position and orientation).

Creating and building a database of fingerprints is not a cumbersome task. As mentioned in [Varshavsky et al. 2007], the time spent in fingerprinting hallways can be very much less than that for following maintenance procedures like elevator servicing, emergency exit lighting etc. Crowdsourcing is the concept that describes a distributed problem solving and product model, in which small tasks are broadcasted to a crowd in the form of open calls for solutions [Alt et al. 2010]. Everyday users engage in activities that help in solving or providing information for a larger context [Eagle 2009]. As part of future work, we plan on integrating this concept to our data collection process around different hallways. In other words, the occupants of the building can collect magnetic signatures of different hallways since they usually move around the same set of locations daily, following routine paths and most of them carry smartphones. The data collected can be uploaded onto a server. This form of data collection and sharing can be also categorized as participatory sensing [Burke et al. 2006] where users can passively participate in the sensing process since all that is required is to walk and collect data. Following the crowdsourcing concept, a database can be built and continuously updated providing accurate maps of the building.

To summarize, this paper showed the possibility of using dynamic time warping for indoor localization. Future work would involve developing a more robust DTW and implementing a real time localization system that can perform classification instantaneously. We also plan to integrate existing landmark based solutions with our work, so that a person's location nearby certain landmarks can be easily provided which could in turn be used for navigating the person to his/her destination. We also plan on devel-

oping a more user friendly application with voice alerts that could be suitable for the blind and visually impaired.

8. RELATED WORK

Many indoor localization systems or solutions exist. They can be grouped based on the types of systems used to provide location estimates: 1) Wearable sensors 2) Infrastructure 3) Ambient sensing 4) Probabilistic and 5) Smartphones. For each category, we highlight the well-known solutions and also list some of the areas where DTW has been applied.

8.1. Wearable sensors

Golding et al [Golding and Lesh 1999] use wearable accelerometer, magnetometer, light and audio sensors to provide indoor localization and navigation. Collin [Collin et al. 2003] propose an indoor positioning system using accelerometers and compasses. Lee [Lee and Mase 2002] develop a dead reckoning based activity and location recognition system. Elena [Vildjiounaite et al. 2002] propose a location estimation system by combining data from wearable sensors and a map. Although pioneering, these solutions require all kinds of electronic circuitry in order to be usable.

8.2. Infrastructure

Cricket [Nissanka et al. 2000] functions through a combination of RF and ultrasound beaconing systems. Active Badge[Want et al. 1992] provides location information using infra red based transmission and reception. Bat system [Addlesee et al. 2001] used ultrasonic location estimation to provide more accurate position data. Another system for location tracking, PlaceLab [Otsason et al. 2005] used signal strength of various wireless connections such as GSM (Global System for Mobile Communications), Bluetooth, and WiFi [Yin et al. 2004]. Randall [Randall et al. 2007] use solar cells combined with an RFID based localization system to determine the user's location. Although these works achieved very fine localization accuracies, they carry with them high installation costs and are not practically feasible for daily use.

8.3. Ambient sensing

Ravi et al [Ravi and Iftode 2007] perform room level localization using light sensors assuming uniform lighting conditions. This assumption may not be valid every time and users' movement is constrained to very slow speeds in order to obtain match. Also the position of the sensor is fixed. Bucur et al [Bucur and Kjrgaard 2008] propose indoor localization system by sensing indoor radioactivity. This work requires specialized sensors not available in smartphones, for both fingerprinting and using as an application. Location fingerprinting based systems surveyed in [Liu et al. 2007] use pattern recognition techniques like k-nearest neighbor, neural networks, probabilistic methods and support vector machines. SkyLoc [Varshavsky et al. 2007] performs floor level localization of different buildings using GSM fingerprinting. RADAR [Bahl and Padmanabhan 2000] uses WiFi fingerprints but requires calibration of signal strengths at many physical locations in the building. A recent work by [Chung et al. 2011] used a compass on a rotating motor to develop an indoor location system using ambient magnetic fields.

8.4. Probabilistic

Probabilistic techniques based particle filters [Arulampalam et al. 2001] have been employed for location estimation using foot mounted inertial sensors [Krach and Roberston 2008; Woodman and Harle 2008], fusing information from multiple sensors [Wendlandt et al. 2006] and using infrared laser range finders, ultrasound sensors [Fox et al. 2003; Hightower and Borriello 2004]. But these are not classification

based systems where the location information is available in a database. Instead they have to be integrated with floor plan information or have to be used with map matching techniques [Bernstein and Kornhauser] to obtain the position estimates. Other methods require calibration which is a burden for the system [Chai and Yang 2007].

8.5. Smartphones

With the proliferation of mobile phones embedded with sensors, various solutions for indoor localization have been on the rise such as those based on activity recognition using accelerometers [Constandache et al. 2010]. However, this work relies on initial GPS and Google Maps for path trails. Accelerometers have also been used for human localization in that a human's daily walking trial is used to locate him. This involves monitoring, collecting and storing every user's movement. Avinash et al [Parnandi et al. 2010] perform coarse localization using a mobile phone's built-in accelerometer by recognizing the walking type. Their idea of using the time taken to walk a particular staircase as a means for localization may not be valid for people walking with different speeds or implementation in all possible buildings. WiFi based fingerprinting and localization using mobile phones has also been attempted [Azizyan and Choudhury 2009]. However, fluctuations in signal strengths, temporary disconnections, maintaining accurate distances from access points during training and testing phases are some of the issues. Ravi et al [Ravi et al. 2006] propose a solution by capturing images with a mobile phone camera. The camera has to be worn as a pendant thereby imposing a placement constraint. Also, building a database of images for all possible locations is cumbersome and may even raise privacy concerns. Authors in [Blankenbach et al. 2011] showed how artificially magnetic fields collected using the built-in magnetometer can be used as a source of indoor positioning.

8.6. Dynamic Time Warping

DTW has been employed as a classifier in some of the existing work. We highlight a few here. Authors in [Muscillo et al. 2007] perform activity recognition by considering variability in speeds and perform classification of motor activities using DTW and derivative DTW. Avinash et al [Parnandi et al. 2010] perform DTW based classification of user activities, however, they do not build upon the classification to provide fine grained location estimates. Grzonka et al [Grzonka et al. 2010] classify motion templates using DTW to perform simultaneous localization and mapping (SLAM). SLAM techniques may not be useful for a common man since a simple localization application should have prior knowledge about the locations in order to accurately locate him indoors. Work in [Gayathri et al. 2011], estimates vehicular speeds through classification of RSS signal strengths of similar looking but time or magnitude varying GSM signals obtained while traveling in a car at different speeds. DTW has also been utilized in power disturbance classification [Youssef et al. 2004], chromosome classification [Legrand et al. 2008], recognition of ECG changes [Tuzcu and Nas 2005]. Tuzcu [Tuzcu and Nas 2005] use DTW algorithm to account for time fluctuations and classify footsteps using the footstep sound.

Overall, the existing work requires sensors to be interfaced with laptops or base stations that have to be placed strategically or systems that pose constraints on the placement and orientation. There is also infrastructure, installation and maintenance cost associated with certain solutions. In contrast to all these existing systems, we developed a fine localization application utilizing just a smartphone. We showed that our work does not pose any placement or orientation constraints, is practically implementable on smartphones with different hardware and most importantly can perform localization *independent of the subject and his/her walking speed.*

9. CONCLUSIONS

Locating a person indoors is an interesting problem in the mobile computing field. By capturing the unique magnetic signatures of different hallways using a smartphone, we exploited the magnetic fields present indoors as a solution to the localization problem. Through analytical modeling we explained the occurrence of magnetic signatures due to different components or sources of disturbances such as pillars, doors, and elevators. Then, by applying time warping technique to the measured magnetic signatures, we showed that our classification framework is independent of the user and also the phone used. Our classification accuracies indicate that hallways can be distinguished with a good success rate. Our low resolution and estimation errors showed the feasibility of our approach. The faster response times, low memory and power consumption indicate the successful implementation of dynamic time warping algorithm on resource limited smartphones.

10. ACKNOWLEDGEMENTS

This work is partially supported by the National Science Foundation under grants CNS-0627754, CNS-0619871 and CNS-0551694. We would also like to thank Dr.Duncan Weathers of the Physics department at UNT for his valuable suggestions.

REFERENCES

Android supported media formats. http://www.android.com.

Application video. http://youtu.be/iHVol1n89TY.

Asahi-kasei. http://www.asahi-kasei.co.jp/asahi/en/news/2006/e070313.html.

The geomagnetic reference model. http://www.ngdc.noaa.gov/IAGA/vmod/igrf.html.

ADDLESEE, M., CURWEN, R., HODGES, S., NEWMAN, J., STEGGLES, P., WARD, A., AND HOPPER, A. 2001. Implementing a sentient computing system. *Computer 34,* 8, 50 –56.

AFZAL, M. H. AND RENAUDIN, V. 2011. Magnetic field based heading estimation for pedestrian navigation environments. In *International Conference on Indoor Positioning and Indoor Navigation (IPIN)*.

ALT, F., SHIRAZI, A. S., SCHMIDT, A., KRAMER, U., AND NAWAZ, Z. 2010. Location-based crowdsourcing: extending crowdsourcing to the real world. In *Proceedings of the 6th Nordic Conference on Human-Computer Interaction: Extending Boundaries*. NordiCHI '10. ACM, New York, NY, USA, 13–22.

ARULAMPALAM, M. S., MASKELL, S., GORDON, N., AND CLAPP, T. 2001. A tutorial on particle filters for online non-linear/non-gaussian bayesian tracking. *IEEE Transactions on Signal Processing 50*, 174–188.

AZIZYAN, M. AND CHOUDHURY, R. R. 2009. Surroundsense: Mobile phone localization using ambient sound and light. *SIGMOBILE Mob. Comput. Commun. Rev. 13*, 69–72.

BAHL, P. AND PADMANABHAN, V. N. 2000. Radar: An in-building rf-based user location and tracking system. In *IEEE INFOCOM*. 775–784.

BERNSTEIN, D. AND KORNHAUSER, A. An introduction to map matching for personal navigation assistants. Tech. rep.

BLANKENBACH, J., NORRDINE, A., HELLMERS, H., AND GASPARIAN, E. 2011. A novel magnetic indoor positioning system for indoor location services. In *Proc. of 8th International Symposium on Location-Based Services*.

BUCUR, D. AND KJRGAARD, M. 2008. *GammaSense: Infrastructureless Positioning Using Background Radioactivity*. Smart Sensing and Context Series, vol. 5279. Springer Berlin / Heidelberg, 69–82.

BURKE, J., ESTRIN, D., HANSEN, M., PARKER, A., RAMANATHAN, N., REDDY, S., AND SRIVASTAVA, M. B. 2006. Participatory sensing. In *In: Workshop on World-Sensor-Web (WSW06): Mobile Device Centric Sensor Networks and Applications*. 117–134.

BURNETT, J. AND YAPING, P. D. 2002. Mitigation of extremely low frequency magnetic fields from electrical installations in high-rise buildings. *Building and Environment 37,* 8-9, 769 – 775.

CHAI, X. AND YANG, Q. 2007. Reducing the calibration effort for probabilistic indoor location estimation. *Mobile Computing, IEEE Transactions on 6,* 6, 649 –662.

CHENG, Y.-C., CHAWATHE, Y., LAMARCA, A., AND KRUMM, J. 2005. Accuracy characterization for metropolitan-scale wi-fi localization. In *Proceedings of the 3rd international conference on Mobile systems, Applications, and Services*. MobiSys '05. ACM, New York, NY, USA, 233–245.

CHUNG, J., DONAHOE, M., SCHMANDT, C., KIM, I.-J., RAZAVAI, P., AND WISEMAN, M. 2011. Indoor location sensing using geo-magnetism. In *Proceedings of the 9th international conference on Mobile systems, applications, and services*. MobiSys '11. ACM, New York, NY, USA, 141–154.

COLLIN, J., MEZENTSVE, O., AND LACHAPELLE, G. 2003. Indoor positioning system using accelerometry and high accuracy heading sensors. In *Proceedings of the 16th International Technical Meeting of the Satellite Division of the Institute of Navigation ION GPS/GNSS*. 796–799.

CONSTANDACHE, I., BAO, X., AZIZYAN, M., AND CHOUDHURY, R. R. 2010. Did you see bob?: human localization using mobile phones. In *Proceedings of the sixteenth annual international conference on Mobile computing and networking*. MobiCom. ACM, New York, NY, USA, 149–160.

CRAIG M. NEWTSON, M. O. E. 1995. Two dimensional magnetic algorithm to detect reinforcing steel. In *Journal of Materials in Civil Engineering*. Vol. 7.

EAGLE, N. 2009. txteagle: Mobile crowdsourcing. In *Internationalization, Design and Global Development*, N. Aykin, Ed. Lecture Notes in Computer Science Series, vol. 5623. Springer Berlin / Heidelberg, 447–456.

E.ČERMÁKOVÁ. 2005. Magnetization of steel building materials and structures in the natural geomagnetic field. *Acta Polytechnica 45,* 6.

EVENNOU, F. AND MARX, F. 2006. Advanced integration of wifi and inertial navigation systems for indoor mobile positioning. *EURASIP J. Appl. Signal Process. 2006*, 164–164.

FOX, V., HIGHTOWER, J., LIAO, L., SCHULZ, D., AND BORRIELLO, G. 2003. Bayesian filtering for location estimation. *Pervasive Computing, IEEE 2,* 3, 24–33.

GAYATHRI, C., TAM, V., ALEXANDER, V., MARCO, G., RICH, M., JIE, Y., AND YINGYING, C. 2011. Tracking vehicular speed variations by warping mobile phone signal strengths. In *IEEE International Conference on Pervasive Computing and Communications (PERCOM), 2011*.

GOLDING, A. R. AND LESH, N. 1999. Indoor navigation using a diverse set of cheap, wearable sensors. *Wearable Computers, The Third International Symposium on*, 29–36.

GOZICK, B., SUBBU, K. P., DANTU, R., AND MAESHIRO, T. 2011. Magnetic maps for indoor navigation. *Instrumentation and Measurement, IEEE Transactions on PP,* 99, 1 –9.

GRZONKA, S., DIJOUX, F., KARWATH, A., AND BURGARD, W. 2010. Mapping indoor environments based on human activity. In *Robotics and Automation (ICRA), 2010 IEEE International Conference on*. 476 –481.

HAVERINEN, J. AND KEMPPAINEN, A. 2009. Global indoor self-localization based on the ambient magnetic field. *Robotics and Autonomous Systems*.

HIGHTOWER, J. AND BORRIELLO, G. 2004. In Particle Filters for Location Estimation in Ubiquitous Computing: A Case Study. *Sixth International Conference on Ubiquitous Computing (Ubicomp)*.

HILL, E. W. AND PUNDER, P. 1976. *Orientation and Mobility Techniques:A Guide for the Practitioner* First Ed. American Foundation for the Blind, 119.

JACKSON, J. D. 1999. *Classical electrodynamics* 3rd ed. Ed. Wiley, New York, NY.

KRACH, B. AND ROBERSTON, P. 2008. Integration of foot-mounted inertial sensors into a bayesian location estimation framework.

KRISTJANSSON, L. 1983. Magnetic field measurements near a steel plate. *European Journal of Physics 4,* 1, 48.

LEE, S.-W. AND MASE, K. 2002. Activity and location recognition using wearable sensors. *Pervasive Computing, IEEE 1; 1,* 3, 24–32.

LEGRAND, B., CHANG, C. S., ONG, S. H., NEO, S.-Y., AND PALANISAMY, N. 2008. Chromosome classification using dynamic time warping. *Pattern Recogn. Lett. 29*, 215–222.

LIU, H., DARABI, H., BANERJEE, P., AND LIU, J. 2007. Survey of wireless indoor positioning techniques and systems. *Systems, Man, and Cybernetics, Part C: Applications and Reviews, IEEE Transactions on 37,* 6, 1067 –1080.

MILLONIG, A. AND SCHECHTNER, K. 2005. Developing landmark-based pedestrian navigation systems. In *Intelligent Transportation Systems, 2005. Proceedings. 2005 IEEE*. 197–202.

MUSCILLO, R., CONFORTO, S., SCHMID, M., CASELLI, P., AND D'ALESSIO, T. 2007. Classification of motor activities through derivative dynamic time warping applied on accelerometer data. In *Engineering in Medicine and Biology Society, EMBS 2007, 29th Annual International Conference of the IEEE*. 4930 –4933.

NISSANKA, P. B., CHAKRABORTY, A., AND BALAKRISHNAN, H. 2000. The cricket location-support system. In *MobiCom '00: Proceedings of the 6th annual international conference on Mobile computing and networking*. ACM Press, New York, NY, USA, 32–43.

OFSTAD, A., NICHOLAS, E., SZCODRONSKI, R., AND CHOUDHURY, R. R. 2008. Aampl: Accelerometer augmented mobile phone localization. *MELT'08 San Francisco, California, USA.*.

OLDENBURG, C. AND MORIDIS, G. 1998. Ferrofluid flow for tough2. Tech. Rep. LBL-41608, Lawrence Berkeley Laboratory, Berkeley.

OTSASON, V., VARSHAVSKY, A., LAMARCA, A., AND DE LARA, E. 2005. Accurate gsm indoor localization. In *In The Proc. of Ubicomp 2005*. 141–158.

PARNANDI, A., LE, K., VAGHELA, P., KOLLI, A., DANTU, K., PODURI, S., AND SUKHATME, G. S. 2010. Coarse in-building localization with smartphones. In *Mobile Computing, Applications, and Services*. Lecture Notes of the Institute for Computer Sciences, Social Informatics and Telecommunications Engineering Series, vol. 35. Springer Berlin Heidelberg, 343–354.

PATHAPATI-SUBBU, K., XU, N., AND DANTU, R. 2009. iknow where you are. In *Social Intelligence and Networking International Symposium 2009, IEEE*.

RANDALL, J., AMFT, O., BOHN, J., AND BURRI, M. 2007. Luxtrace: indoor positioning using building illumination.

RAVI, N. AND IFTODE, L. 2007. Fiatlux: Fingerprinting rooms using light intensity.

RAVI, N., SHANKAR, P., FRANKEL, A., ELGAMMAL, A., AND IFTODE, L. 2006. Indoor localization using camera phones. In *Mobile Computing Systems and Applications, 2006. WMCSA '06. Proceedings. 7th IEEE Workshop on*. 19.

ROETENBERG, D., LUINGE, H., AND VELTINK, P. 2003. Inertial and magnetic sensing of human movement near ferromagnetic materials. In *Proceedings of the Second IEEE and ACM International Symposium on Mixed and Augmented Reality*. 268–269.

STORMS, W. F. AND RAQUET, J. F. 2009. Magnetic field aided indoor navigation. In *Proceedings of the 13th European Navigation Conference GNSS*.

SUBBU, K., GOZICK, B., AND DANTU, R. 2011. Indoor localization through dynamic time warping. In *Systems, Man, and Cybernetics (SMC), 2011 IEEE International Conference on*. 1639 –1644.

TUZCU, V. AND NAS, S. 2005. Dynamic time warping as a novel tool in pattern recognition of ecg changes in heart rhythm disturbances. In *Systems, Man and Cybernetics, 2005 IEEE International Conference on*. Vol. 1. 182 – 186 Vol. 1.

VARSHAVSKY, A., LAMARCA, A., HIGHTOWER, J., AND DE LARA, E. 2007. The skyloc floor localization system. In *Pervasive Computing and Communications, 2007. PerCom '07. Fifth Annual IEEE International Conference on*. 125 –134.

VILDJIOUNAITE, E., MALM, E.-J., KAARTINEN, J., AND ALAHUHTA, P. 2002. Location estimation indoors by means of small computing power devices, accelerometers, magnetic sensors, and map knowledge. In *Pervasive Computing*, F. Mattern and M. Naghshineh, Eds. Lecture Notes in Computer Science Series, vol. 2414. Springer Berlin / Heidelberg, 5–12.

WANT, R., HOPPER, A., FALCÃO, V., AND GIBBONS, J. 1992. The active badge location system. *ACM Trans. Inf. Syst. 10*, 91–102.

WENDLANDT, K., KHIDER, M., ANGERMANN, M., AND ROBERTSON, P. 2006. Continuous location and direction estimation with multiple sensors using particle filtering. In *Multisensor Fusion and Integration for Intelligent Systems, 2006 IEEE International Conference on*. 92–97.

WOODMAN, O. AND HARLE, R. 2008. Pedestrian localisation for indoor environments. In *UbiComp '08: Proceedings of the 10th international conference on Ubiquitous computing*. ACM, New York, NY, USA, 114–123.

YAMAZAKI, K., KATO, K., ONO, K., SAEGUSA, H., TOKUNAGA, K., IIDA, Y., YAMAMOTO, S., ASHIHO, K., FUJIWARA, K., AND TAKAHASHI, N. 2003. Analysis of magnetic disturbance due to buildings. *Magnetics, IEEE Transactions on 39,* 5, 3226 – 3228.

YIN, J., CHAI, X., AND YANG, Q. 2004. High-level goal recognition in a wireless lan. In *AAAI'04*. 578–584.

YOUSSEF, A., ABDEL-GALIL, T., EL-SAADANY, E., AND SALAMA, M. 2004. Disturbance classification utilizing dynamic time warping classifier. *Power Delivery, IEEE Transactions on 19,* 1, 272 – 278.

ZHENG, Y. AND XIE, X. 2011. Learning travel recommendations from user-generated gps traces. *ACM Trans. Intell. Syst. Technol. 2,* 1, 2:1–2:29.